

# Morphological Characterization of the Core–Shell Latex Particle by Transmission Electron Microscopy and Image Analysis

Zhengmin Li,<sup>1,2</sup> Jinghe Yang,<sup>1</sup> Yuanzhang Yu,<sup>2</sup> Xingzhong Xu,<sup>2</sup> Xiantan Meng,<sup>2</sup> Weijun Yu,<sup>2</sup> Xiuling Xu,<sup>2</sup> Lei Li,<sup>1</sup> Xiuying Yue<sup>2</sup>

<sup>1</sup>School of Chemistry and Chemical Engineering, Shandong University, Jinan 250100, People's Republic of China

<sup>2</sup>Research Institute of Qilu Petrochemical Corporation, Zibo 255400, People's Republic of China

Received 15 July 2002; accepted 21 October 2002

**ABSTRACT:** To describe the morphology of the core–shell latex particle of methyl methacrylate–butadiene–styrene graft copolymer (MBS) quantitatively, we propose four parameters, that is, the diameter of the core, the shell thickness (TH), the roundness of the core, and the eccentricity ( $E$ ); we calculated these parameters with geometrical parameters determined by the analysis of transmission electron microscope images. The mean values and distributions of the four parameters based on a certain amount of particles were used for quantitative characterization of MBS latex samples. With increasing monomer-to-polymer ratios of the graft polymer-

ization, both the MBS TH and the numbers of homopolymer particles increased, and the core–shell morphology tended to be irregular. For the MBS latices derived from poly(styrene–butadiene) latex with a wide distribution of particle sizes, the core–shell structures of the larger particles were different from those of smaller ones to a certain extent, and both the TH and the  $E$  decreased with increasing core size. © 2003 Wiley Periodicals, Inc. *J Appl Polym Sci* 89: 855–861, 2003

**Key words:** core–shell polymers; morphology; TEM; imaging

## INTRODUCTION

Methyl methacrylate–butadiene–styrene graft copolymer (MBS) is known as one of the most efficient transparent impact-resistance modifiers for poly(vinyl chloride) (PVC) resin. The particle size of the rubber and its adhesion with the matrix are two factors involved in the rubber toughening of glassy polymers. Consequently, a typical MBS particle is often designed to have an elastomeric core of a random styrene (St)–butadiene copolymer and a glassy shell composed of a random copolymer of St and methyl methacrylate (MMA).<sup>1,2</sup> A perfect shell would ensure interface between the rubber cores with the PVC matrix for good adhesion during application. Therefore, the core size, the shell thickness (TH), and the uniformity of the graft layer are thought to have close relationship with the properties of PVC/MBS blends.<sup>1,3,4</sup> MBS latex can be synthesized by emulsion polymerization techniques.<sup>5,6</sup> An irregular core–shell structure is frequently formed in which the core is not a circle and/or not at the center of MBS particle. Therefore, to investigate the effect of graft polymerization on the core–shell structure, it is necessary to characterize it quantitatively.

Control and characterization of the core–shell structure are important for many composite latices used as adhesives, coatings, and impact modifiers. The particle size of a latex can be determined by many methods and instruments, including laser light scattering and centrifugal sedimentation.<sup>7–9</sup> However, the core–shell structures cannot be determined directly by these methods. Although the core size and TH of a few particles with a uniform core–shell structure can be manually measured based on their transmission electron microscopy (TEM) images, it is impossible to determine the structures of a sufficient number of irregular core–shell latex particles. The morphology of the core–shell latex particle is generally described with TEM imaging.<sup>10–12</sup> However, this method is imprecise and qualitative. Recently, the shape factor method, which is sensitive to particle shape, has been used to characterize the particle shape of powders.<sup>13–15</sup> However, quantitative characterization of the core–shell morphology of a latex with the shape factor method has rarely been reported in the published literature.

In this study, we chose the diameter of the core ( $D_{\text{core}}$ ) and the TH to represent the size of the MBS particle. Two shape factors, that is, the roundness of core ( $R_{\text{core}}$ ), and eccentricity ( $E$ ), are proposed and were used to characterize the uniform degree of the core–shell structure. The mean value and distribution of these four parameters were used for quantitative characterization of the MBS latex samples. All of the

Correspondence to: J. Yang (yjh@sdu.edu.cn).

**TABLE I**  
**Basic Experimental Recipe**

	MBS-1	MBS-2	MBS-3	MBS-4
H <sub>2</sub> O	300	300	300	300
SBL (solid)	SBL-1	SBL-2	SBL-2	SBL-2
	65	55	45	35
St	17.5	22.5	27.5	32.5
MMA	17.5	22.5	27.5	32.5
Potassium oleate/M (%)	1.0	1.0	1.0	1.0
Crosslinking agent/M (%)	1.5	1.5	1.5	1.5
Redox initiator/M (%)	0.5	0.5	0.5	0.5

M = monomer. A weight ratio was used.

parameters were determined and calculated by the analysis of TEM images. The influence of the monomer-to-polymer ratio and poly(styrene-butadiene) latex (SBL) particle size on the MBS core-shell structure was investigated.

## EXPERIMENTAL

### Preparation of MBS latex samples

MBS latices were prepared by seeded two-stage emulsion polymerization, which has been reported in the literature.<sup>5,6</sup> In this study, the graft polymerization was conducted in a 5-liter stainless steel reactor in a nitrogen atmosphere. SBL and an aqueous solution of potassium oleate were fed into the reactor. Half of the mixture of St monomer, redox initiator, and crosslinking agent was charged to the reactor. The stirring speed of the two-curved blade impeller was 300 rpm, and the polymerization temperature was 60°C. About 1 h later, the other half of the mixture was charged. After 5 h of the graft polymerization of St, the MMA monomer, with initiator and crosslinking agent, was charged to the reactor in two batches at an interval of 1 h. The graft polymerization of MMA continued for 6 h. The four MBS latices were synthesized according to the recipe shown in Table I.

### TEM specimen preparation and the acquisition of TEM image

MBS latices were diluted with deionized water until the proper concentration was reached. A drop of the diluted MBS latex was placed on a TEM grid with Formvar film, and the grid was exposed to osmium tetroxide vapor for about 1 h at room temperature. Osmium tetroxide selectively attacked the carbon-carbon double bonds of the polybutadiene component, so that rubber cores were stained and hardened. However, the shell layers without the carbon-carbon double bonds could not be stained.

Core-shell morphology was observed with a Hitachi H-7000 transmission electron microscope (Tokyo, Japan) at a magnification of 80,000 $\times$ . TEM images of the four MBS latex samples are shown in Figure 1, in which the cores are in black and the shells are in gray. Twenty images were acquired with a Kodak charge coupled device (CCD) camera (1280  $\times$  1024 pixels), and the magnifications were calibrated by a standard grating replica (2160 lines/mm).

### Processing of TEM images and measurement of the geometrical parameters

In this work, SIS Analysis 3.0 software (Münster, Germany) was used to process and detect the images, and Excel 2000 software (Washington, USA) was used for both data handling and graph drawing. All of the geometrical parameters were evaluated on the basis of a projected image of randomly positioned particles.

As an example of TEM image, Figure 1(c) is a two-dimensional array of 1280  $\times$  1024 pixels (picture elements) with gray values from 0 to 255. To enable the system to distinguish the MBS cores from both the background and the MBS shell during the measurement, a gray value range (threshold) was selected so that pixels of the MBS cores were in the range and pixels of both background and MBS shells were out of it. After the gray-value image was transformed into a binary image that had only two gray values, 0 (black) or 255 (white), the MBS cores were in white, and both the shell and background were in black [Fig. 2(a)].

Another gray range was selected so that both the MBS cores and shell were in white and the background was in black. Some particles in the original image touched with each other. This made the detection of these particles impossible. After applying the separate particles filter, the particles were separated [Fig. 2(b)]. All particles cut by the image border were excluded because their images did not have integrity.

The geometrical parameters of both MBS particles and their cores were determined. The core parameters included area ( $A$ ), perimeter ( $P$ ), equivalent circle diameter ( $D_{\text{core}}$ ), and the coordinates of the center ( $X_{\text{core}}$ ,  $Y_{\text{core}}$ ). The MBS particle parameters were equivalent circle diameter ( $D_{\text{MBS}}$ ) and the coordinates of the center ( $X_{\text{MBS}}$  and  $Y_{\text{MBS}}$ ), where the equivalent circle diameter is the diameter of a circle that has an  $A$  equal to the  $A$  of the particle and the coordinates of the center is the average of the coordinates of all of the pixels in the particle.

These procedures of image processing and measurement were combined into a macro program. By running it, we could process the other images automatically.

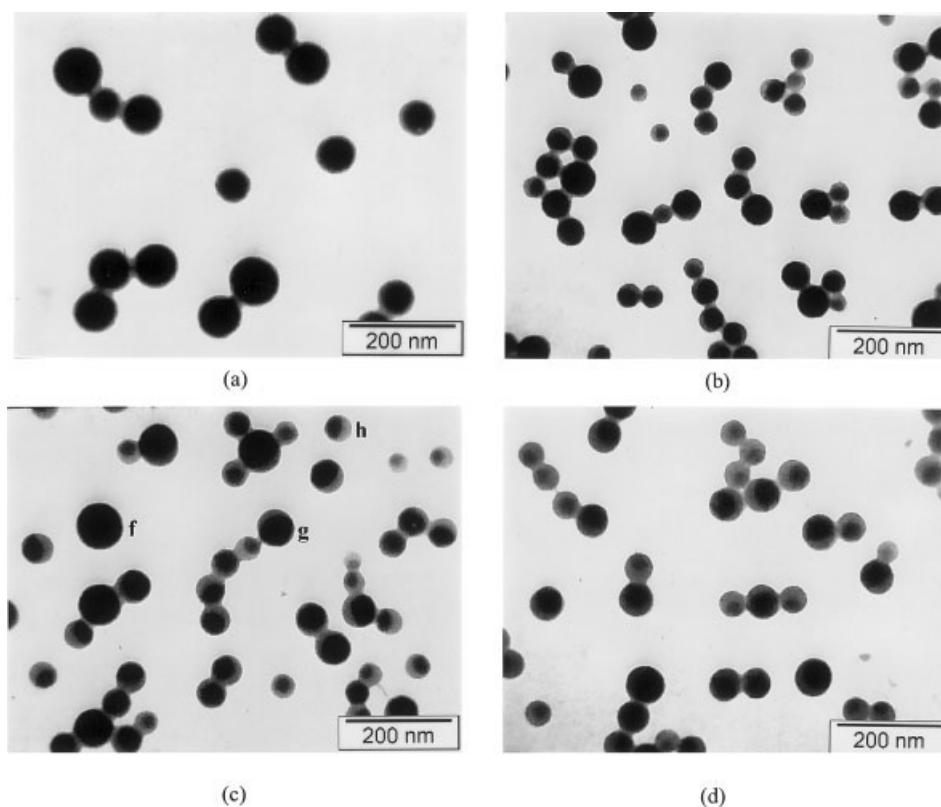


**Figure 1** TEM images of MBS latices stained with osmium tetroxide. Dark regions are cores, and gray regions are shell layers. (a) MBS-1, (b) MBS-2, (c) MBS-3, and (d) MBS-4 were synthesized by graft polymerization at monomer-to-polymer ratios of 0.54, 0.82, 1.22, and 1.86, respectively. MBS-1 was derived from large-particle SBL and the others were derived from small-particle SBL.

## RESULTS AND DISCUSSION

### Parameters used to characterize the core-shell structure of MBS latex particles

Two kinds of parameters were essential to characterize the MBS core-shell structure quantitatively. The first kind was used to represent the size; here,  $D_{\text{core}}$  and TH of the MBS particle were chosen. TH can be calculated by eq. (1):

$$TH = \frac{1}{2}(D_{\text{MBS}} - D_{\text{core}}) \quad (1)$$

The second kind of parameter was used to describe the shape. On the basis of the typical core-shell structures of the MBS particles in Figure 1, roundness ( $R$ ) was chosen, and  $E$  was designed.

$R$ , which is frequently used to describe the degree to which a particle approaches a circle, is defined as the

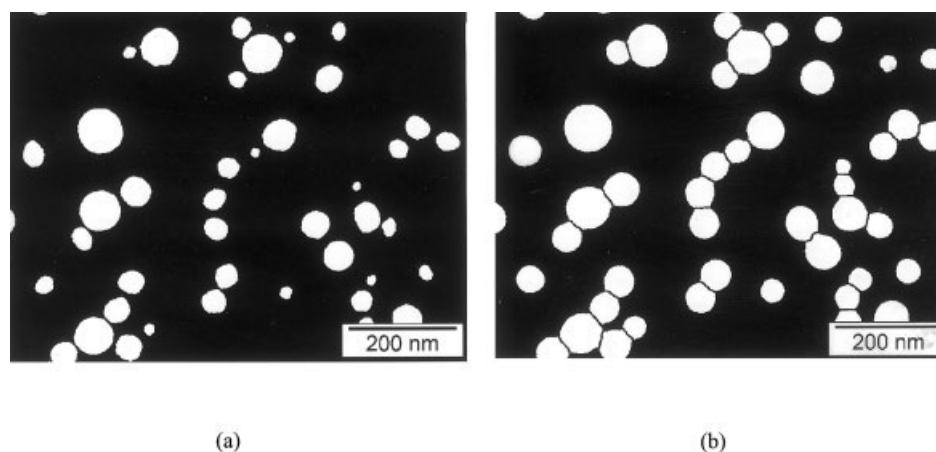


**Figure 2** Binary images of Figure 1(c). The white regions are (a) MBS cores and (b) whole MBS particles.

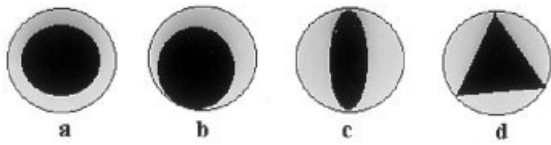


**Figure 3** Model particles with special core-shell structures.

ratio of the  $A$  of the particle's projected image to the circle  $A$  that has the same  $P$ . The formula for this calculation is:

$$R = \frac{4\pi A}{P^2} \quad (2)$$

The values of  $R$  equal 1 for a spherical particle and are near 0 for a line particle. For all other particles, they are more than 0 and less than 1.

In geometry,  $E$  is often used as a geometric parameter of an ellipse and is defined as the ratio of the difference in length between the major axis and minor axis to the length of the major axis. However, to represent the degree that the center of core deviated from that of the whole MBS particle, we defined  $E$  as the ratio of the distance between the center of the core ( $X_{\text{core}}, Y_{\text{core}}$ ) and that of the whole particle ( $X_{\text{MBS}}, Y_{\text{MBS}}$ ) to the equivalent circle radius ( $1/2 D_{\text{MBS}}$ ) of the whole MBS particle, that is

$$E = \frac{2\sqrt{(X_{\text{core}} - X_{\text{MBS}})^2 + (Y_{\text{core}} - Y_{\text{MBS}})^2}}{D_{\text{MBS}}} \quad (3)$$

The  $E$  value equals 0 when the two centers of the core and MBS are identical, and when the center of core is far away from that of MBS,  $E$  is close to 1.

All of the MBS particles with a single core were generally close to spherical in water because of the action of the surface tension, so the  $R$  of MBS particle was not taken into account. Each MBS particle had a unique value of  $D_{\text{core}}$ , TH,  $R_{\text{core}}$ , and  $E$ , in which  $D_{\text{core}}$  and TH represented the size of the MBS particle accurately and  $R_{\text{core}}$  and  $E$  reflected the principal shape character of the core-shell morphology. For a perfect core-shell structure,  $R_{\text{core}}$  would be equal to 1 and  $E$  would be equal to 0.

#### Determination of the four parameters of individual MBS particles

Microscopy is one of the basic methods of particle size measurement. However, it is tedious to observe and detect a large number of particles, so its application is limited. Analysis of microscopic images can do this job easily and has been used as an ASTM standard to determine particle size.<sup>8,16</sup> This method can reach a better accuracy in the course of application.<sup>9,17</sup> Thus,  $D_{\text{core}}$  and TH, where the latter is derived from the

former and DMBS, can be accurately determined by TEM image analysis.

After the images of the four model particles ( $a$ ,  $b$ ,  $c$ , and  $d$ ), drawn by computer (Fig. 3), and the three true particles ( $f$ ,  $g$ , and  $h$ ) in Figure 1(c) were processed, the  $D_{\text{core}}$  and other parameters of each particle were determined, respectively.

The values of TH,  $R_{\text{core}}$ , and  $E$  were calculated according to eqs. (1–3). The results are shown in Table II. Model particle  $a$  has a perfect core-shell structure, so its  $R_{\text{core}}$  equals 1 and  $E$  equals 0. The core of model particle  $b$  is a circle, but its center deviates from the center of the whole particle, so its  $R_{\text{core}}$  equals 1 and its  $E$  is greater than 0. On the contrary, the centers of model particles  $c$  and  $d$  are nearly coincident with their core centers. However, the two cores are not circles. So their  $E$  values are near 0, and their  $R_{\text{core}}$  values are smaller than 1. The  $R_{\text{core}}$  value of particle  $f$  was the maximum, and that for particle  $h$  was the minimum among three true particles shown in Figure 1(c). The  $E$  value of particle  $f$  was the minimum, and that of particle  $h$  was the maximum. These results are agreeable to those observed from the image.

#### Determination of the mean values and distributions of the four parameters

The four parameters ( $D_{\text{core}}$ , TH,  $R_{\text{core}}$ , and  $E$ ) of the individual particles were obtained with the previously discussed method. However, our concern was with the whole sample, not with individual particles. So the mean value and distribution of the four parameters of a large number of randomly positioned particles were used to characterize the core-shell structure of the whole sample in this study.

For the determination of the particle size and the shape factor, an average number of at least 500 particles or 5–20 micrographs is recommended.<sup>9,16,17</sup> Therefore, the determination of mean values and distributions were based on 20 TEM images; that is, about 500 particles were detected.

The mean diameter of the core ( $\overline{D_{\text{core}}}$ ), mean shell thickness ( $\overline{\text{TH}}$ ), mean roundness ( $\overline{R_{\text{core}}}$ ), and mean eccentricity ( $\overline{E}$ ), which were based on particle numbers, of the four MBS samples were calculated and are

**TABLE II**  
Values of  $D_{\text{core}}$ , TH,  $R_{\text{core}}$ , and  $E$  of the Four Model Particles ( $a$ ,  $b$ ,  $c$ , and  $d$ ) Drawn by Computer (Fig. 3) and the Three True Particles [ $f$ ,  $g$ , and  $h$ ; Fig. 1(c)]

Parameter	$a$	$b$	$c$	$d$	$f$	$g$	$h$
$D_{\text{core}}$ (nm)	—	—	—	—	72	51	24
TH (nm)	—	—	—	—	4.0	6.3	10.7
$R_{\text{core}}$	1.00	1.00	0.73	0.63	0.95	0.87	0.73
$E$	0.00	0.10	0.00	0.03	0.01	0.05	0.13

**TABLE III**  
Parameter Values of MBS Samples

Sample	$\overline{D_{core}}$ (nm)	$\overline{TH}$ (nm)	$\overline{R_{core}}$	$\overline{E}$	Homopolymer particles (%)
MBS-1	60	3.7	0.89	0.022	2
MBS-2	35	4.3	0.89	0.064	15
MBS-3	36	5.9	0.86	0.095	16
MBS-4	34	7.7	0.82	0.107	22

listed in Table III. The distributions of the core size and TH are plotted in Figures 4 and 5, respectively.

As shown in Figure 4, the  $D_{core}$  of some particles was equal zero. These particles “without cores” were the homopolymer of either MMA or St. The percentages of homopolymer particles to the total are listed in Table III also; this value could be used as a parameter to describe the MBS latices.

**Comparison between MBS with a perfect core-shell structure and MBS with an irregular structure**

As shown in Figures 4 and 5, MBS-1 had a narrower distribution than MBS-2, MBS-3, or MBS-4 for both core size and TH. The percentages of particles without cores in MBS-2, MBS-3, or MBS-4 were greater than that in MBS-1. This means that there were more graft monomers to form homopolymer during the graft polymerization for MBS-2, MBS-3, and MBS-4. As shown in Table III, the mean roundness ( $\overline{R_{core}}$ ) of MBS-1 was larger than that of MBS-2, MBS-3, or MBS-4 in the main, and the mean eccentricity ( $\overline{E}$ ) of MBS-1 was less than that of the other samples.

As seen in Figure 6, the majority of the MBS-1 particles, approximately 90%, possessed  $R_{core}$  values in the range 0.9–1.0 and  $E$  values in the range 0–0.1. However, the two shape factors of most MBS-2, MBS-3, and MBS-4 particles were in a wider range, with  $R_{core}$  values between 0.7 and 1.0 and  $E$  values between 0 and 0.2. In comparison with MBS-2, MBS-3,

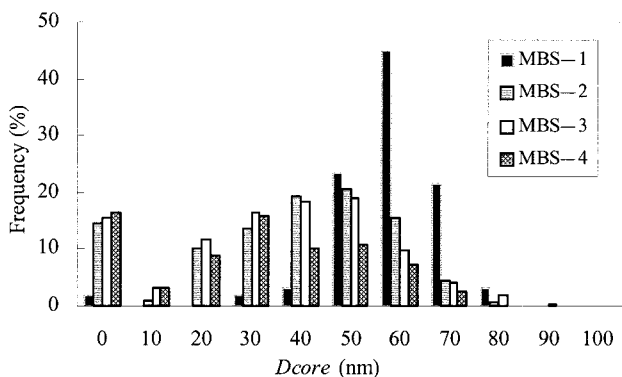


**Figure 4** Core-size distributions of MBS-1, MBS-2, MBS-3, and MBS-4.

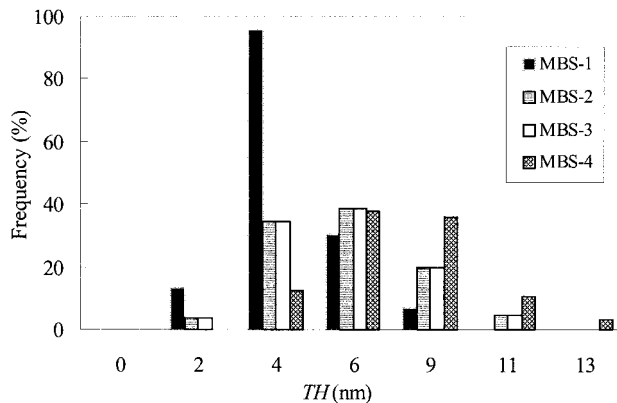


**Figure 5** TH distributions of MBS-1, MBS-2, MBS-3, and MBS-4.

and MBS-4, the  $R_{core}$  and  $E$  values of MBS-1 were closer to 1.0 and 0, respectively. The results indicate that particles of MBS-1 had a more perfect core-shell structure, which was compatible with what we saw when we carefully examined the TEM images. However, it was difficult to find slight changes in the core-shell structure of the MBS latex with TEM observation.

**Effect of the monomer-to-polymer ratio on the core-shell structure**

The core-shell structure of latex may be influenced by many factors.<sup>18,19</sup> In this study, the effect of monomer-to-polymer ratio on core-shell structure was examined. As shown in Table I, the monomer-to-polymer ratios of MBS-1, MBS-2, MBS-3, and MBS-4 were 0.54, 0.82, 1.22, and 1.86, respectively. As shown in the data presented in Table III, from MBS-1, MBS-2, and MBS-3 to MBS-4, TH,  $E$ , and the percentages of homopolymer increased, whereas  $R_{core}$  decreased. The results mean that with increasing monomer-to-polymer ratios, the perfect degree of core-shell structure decreased, and

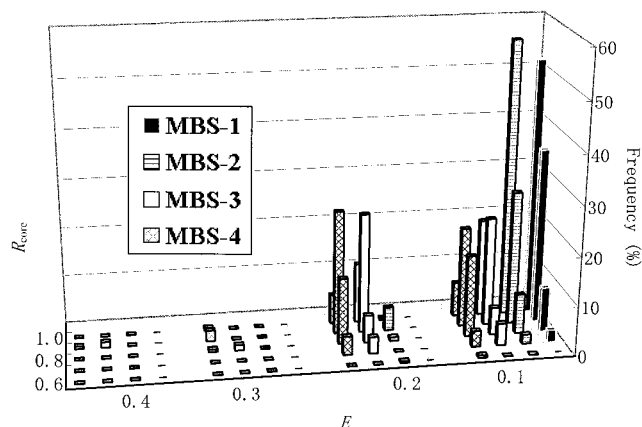


**Figure 6** Shape factor distribution of MBS-1, MBS-2, MBS-3, and MBS-4.

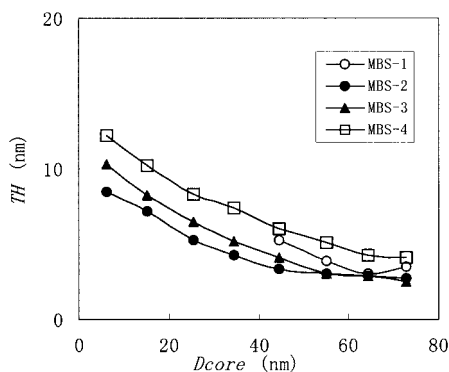


Figure 7 Relationship between TH and  $D_{core}$ .

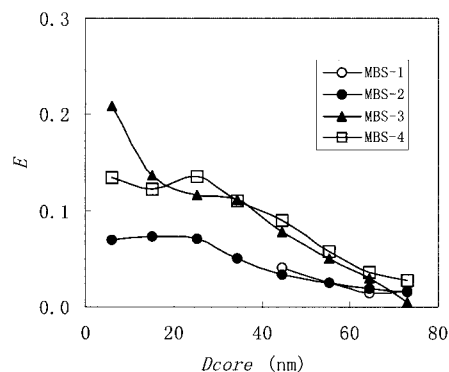


Figure 9 Relationship between  $E$  and  $D_{core}$ .

the shell became thicker. In high concentrations of the monomers, there were two kinds of reactions during graft polymerization: one was the graft polymerization of the monomers onto SBL, and the other was the self-polymerization of monomers, which resulted in an increase in the percentages of homopolymer. So the MBS latex with a thin, perfect shell, and a small amount of homopolymer particles was obtained at a lower monomer-to-polymer ratio.

#### Relationship between the core-shell structure and the MBS core size for one latex emulsion

Li<sup>20</sup> studied the graft polymerization of latices with different mean particle sizes. However, the difference in the core-shell structure of MBS latex particles derived from large and small particles of one SBL emulsion with a wide particle-size distribution still needed to be investigated. As shown by the core-size distributions of MBS-2, MBS-3, and MBS-4 (Fig. 4), the diameters of the larger particles were about two to four times greater than those of the smaller ones. As shown in Figures 7–9, with increasing core size in MBS-2, MBS-3, and MBS-4, TH decreased gradually, and  $R_{core}$  increased a little, but  $E$  decreased obviously. The same trend also appeared in MBS-1, although its particle-size distribution was narrower.

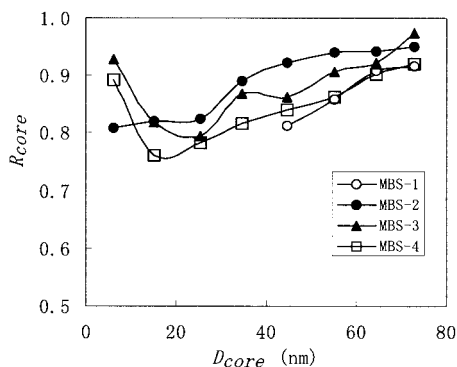


Figure 8 Relationship between  $R_{core}$  and  $D_{core}$ .

From the previous quantitative characterization of MBS particles, we concluded that the graft effect of larger particles was different from that of smaller ones for SBL with a wide particle-size distribution. The SBL with larger diameter and narrower particle-size distribution tended to form a perfect and thin-shell layer during graft polymerization under the same conditions. This conclusion was also proven by the facts that the core-size distribution of MBS-1 was narrow and its shell was uniform.

#### CONCLUSIONS

Four parameters,  $D_{core}$ , TH,  $R_{core}$ , and  $E$  were proposed or designed to characterize core-shell structure of the MBS latex particle quantitatively, where  $D_{core}$  and TH represent the size of MBS particle accurately and  $R_{core}$  and  $E$  reflect the principal shape character of core-shell structure. These parameters were calculated with geometrical parameters determined by the analysis of TEM images. The mean value and distribution of the four parameters based on a large number of particles described the particle size and morphology of the MBS latex samples quantitatively.

With increasing monomer-to-polymer ratios, both TH and the numbers of homopolymer particles increased, and the core-shell morphology tended to be irregular. The core-shell structures of the MBS particles derived from the variously sized SBL particles were different, and with increasing core size, both TH and  $E$  decreased.

#### References

1. Takaki, A.; Yasui, H. *Polym Eng Sci* 1997, 37, 105.
2. Dompas, D.; Groeninckx, G.; Isogawa, M.; Hasegawa, T.; Kadokura, M. *Polymer* 1995, 36, 437.
3. Dompas, D.; Groeninckx, G.; Isogawa, M.; Hasegawa, T.; Kadokura, M. *Polymer* 1994, 35, 4760.
4. Wu, P. X.; Zhang, L. C. *Blend Modification of Polymer*; China Light Industry Press: Beijing, China, 1992; p 98.

5. Lu, X.; Zhang, L.; Yu, Y. Z.; Sun, H. Y.; Luan X. S. *Sci Technol Chem Ind* 1999, 7, 39.
6. Zhao, J. Q.; Yuan, H. Z.; Pan, Z. R. *J Appl Polym Sci* 1994, 53, 1447.
7. Howard, G. B.; Sun, S. T. *Anal Chem* 1993, 65, 55r.
8. Allen, T. *Particle Size Measurements*, 3rd ed.; Chapman & Hall: London, 1981; p 107.
9. Li, Z. M.; Yu, W. J.; Xu, X. L.; Yue, X. Y.; Liu, Y. X. *China Powder Sci Technol* 2000, 3, 32.
10. Lee, D. I.; Ishikawa, T. *J Polym Sci Polym Chem Ed* 1983, 21, 147.
11. Chen, Y. C.; Dimonie, V.; El-Aasser, M. S. *J Appl Polym Sci* 1992, 46, 691.
12. Chen, Y. C.; Dimonie, V.; El-Aasser, M. S. *J Appl Polym Sci* 1992, 45, 478.
13. Li, Z. M.; Yang, J. H.; Xu, X. Z.; Xu, X. L.; Yu, W. J.; Yue, X. Y.; Sun, C. X. *Adv Powder Technol* 2002, 13, 249.
14. Miyajima, T.; Yamamoto, K.; Sugimoto, M. *Adv Powder Technol* 2001, 12, 117.
15. Podczeczek, F. *Powder Technol* 1997, 93, 47.
16. ASTM Standard E 1382-91. *Annu Book ASTM Stand* 1991, 03(01), 855.
17. Vigneau, E.; Loisel, C.; Devaux, M. F.; Cantoni, P. *Powder Technol* 2000, 107, 243.
18. Merkel, M. P.; Dimonie, V. L.; El-Aasser, M. S.; Vanderhoff, J. W. *J Polym Sci Part A: Polym Chem* 1987, 25, 1755.
19. Kan, C. Y.; Kong, X. Z.; Yuan, Q.; Liu, D. *J Appl Polym Sci* 2001, 80, 2251.
20. Li, L. Q. *China Synth Rubber Ind* 1998, 21, 344.